11

Advanced (Non-traditional) Machining Processes

V.K. Jain

Department of Mechanical Engineering, Indian Institute of Technology Kanpur, Kanpur-208016, India.
E-mail: vkjain@iitk.ac.in

While making a part from raw material, one may require bulk removal of material, forming cavities/holes and finally finishing as per the parts requirements. Many advanced finishing processes have been employed to make circular and/or non-circular cavities and holes in difficult-to-machine materials. Some of the processes employed for hole making are electro-discharge machining, laser beam machining, electron beam machining, shaped tube electro-chemical machining and electro-chemical spark machining. With the demand for stringent technological and functional requirements of the parts from the micro- to nanometre range, ultra-precision finishing processes have evolved to meet the needs of the manufacturing scientists and engineers. The traditional finishing processes of this category have various limitations, for example, complex shapes, miniature sizes, and three-dimensional (3D) parts cannot be processed/finished economically and rapidly by traditional machining/finishing processes. This led to the development of advanced finishing techniques, namely abrasive flow machining, magnetic abrasive finishing, magnetic float polishing, magneto-rheological abrasive finishing and ion beam machining. In all these processes, except ion beam machining, abrasion of the workpiece takes place in a controlled fashion such that the depth of penetration in the workpiece is a small fraction of a micrometre so that the final finish approaches the nano range. The working principles and the applications of some of these processes are discussed in this chapter.

11.1 Introduction

The expectations from present-day manufacturing industries are very high, *viz.* high economic manufacturing of high-performance precision and complex parts made of very hard high-strength materials. Every customer demands products to their own taste/choice, hence there is a need for high-quality low-cost parts made in small batches and large variety. Furthermore, there is a trend in the market for miniaturization of parts with high degree of reliability. The traditional machining methods, even with added CNC features, are unable to meet such stringent demands of various industries such as aerospace, electronics, automobiles, *etc*. As a result, a new class of machining processes has evolved over a period of time to meet such demands, named non-traditional, unconventional, modern or advanced machining processes [1–3]. These advanced machining processes (AMP) become still more important when one considers precision and ultra-precision machining. In some AMPs, material is removed even in the form of atoms or molecules individually or in groups. These advanced machining processes are based on the direct application of energy for material removal by mechanical erosion, thermal erosion or electro-chemical/chemical dissolution.

Developments in materials science have led to the evolution of difficult-to-machine, high-strength temperature-resistant materials with many extraordinary qualities. Nanomaterials and smart materials are the demands of the day. To make different products in various shapes and sizes, traditional manufacturing techniques are often found not fit for purpose. One needs to use non-traditional or advanced manufacturing techniques in general and advanced machining processes in particular [1]. The latter includes both bulk material removal advanced machining processes as well as advanced fine finishing processes. Bulk material removal activities can be divided mainly in two categories, hole or cavity making, and shaping. Furthermore, the need for high precision in manufacturing was felt by manufacturers the world over, to improve interchangeability of components, enhance quality control and increase wear/fatigue life [4, 5].

The first three sections of this chapter deal with the working principles and parametric analysis of some of the important hole making and shaping processes, and some of the applications of each of them. The last section deals with some of the advanced fine finishing processes and their special applications. Figure 11.1 shows the classification of various AMP. In mechanical-type AMP, a mechanical force is employed to remove/erode material from the workpiece. In thermo-electric/thermal processes, it is the heat that is responsible for the thermal erosion of material from the workpiece surface. In electro-chemical and chemical machining processes, it is an electro-chemical or chemical reaction that removes material from the workpiece. Only a few of these processes are discussed, in brief, in this chapter. Furthermore, none of these processes is unique such that it can be satisfactorily employed in all machining situations.

Shaping and sizing are not the only requirements of a part. Surface integrity in general, and surface finish in particular, is equally important. Traditionally, abrasives either in loose or bonded form whose geometry varies continuously in an unpredictable manner during the process are used for final finishing purposes. Nowadays, new advances in materials syntheses have enabled the production of ultra-fine abrasives in the nanometre range. With such abrasives, it has become possible to achieve nanometre surface finishes and dimensional tolerances. There are processes (ion beam machining and elastic emission machining) that can give ultra-precision finish of the order of size of an atom or molecule of a substance. In some cases, the surface finish (center line average (CLA) value) obtained has been reported to be even smaller than the size of an atom. Various processes have been

Classification of advanced machining Processes

Mechanical advanced machining processes

Bulk material removal processes
- Abrasive jet machining (AJM)
- Ultrasonic machining (USM)
- Water jet machining (WJM)
- Abrasive water jet machining (AWJM)

Micro/nanofinishing processes
- Abrasive flow machining (AFM)
- Magnetic abrasive finishing (MAF)
- Magneto-rheological finishing (MRF)
- Magneto-rheological abrasive flow finishing (MRAFF)
- Magnetic float polishing (MFP)
- Elastic emission machining (EMM)
- Ion beam machining (IBM)

Thermal advanced machining processes

- Plasma arc machining (PAM)
- Laser beam machining (LBM)
- Electron beam machining (EBM)
- Electro-discharge machining (EDM)

Electro-chemical and chemical advanced machining processes

- Electrochemical machining (ECM)
- Chemical machining (ChM)
- Biochemical machining (BM)

Figure 11.1. Classification of advanced machining processes

employed for finishing purposes, like abrasive flow machining (AFM), magnetic abrasive flow machining (MAFM), magnetic abrasive finishing (MAF), magnetic float polishing (MFP), magneto-rheological abrasive flow finishing (MRAFF), elastic emission machining (EEM) and ion beam machining (IBM).

11.2 Mechanical Advanced Machining Processes (MAMP)

Mechanical-type advanced machining processes (MAMP) are of various types, as shown in Figure 11.1. This section deals with two commonly used MAMP, *viz*. ultrasonic machining (USM) and abrasive water jet cutting (AWJC).

11.2.1 Ultrasonic Machining (USM)

The ultrasonic machining (USM) process is normally employed for hard and/or brittle materials (irrespective of their electrical conductivity) usually having hard-

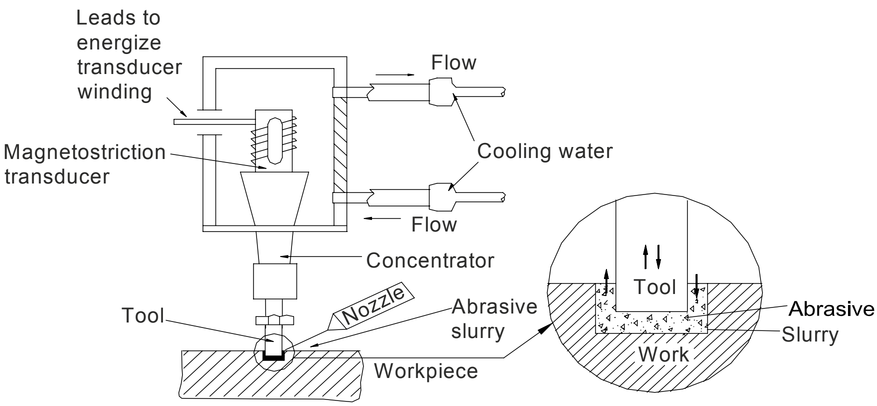

Figure 11.2. A schematic diagram of ultrasonic machining

ness > 40 RC. As shown in Figure 11.2, a slurry (a mixture of fine abrasive particles and water) is supplied in the gap between tool and workpiece [1]. The tool vibrates at a very high frequency (≥ 16 kHz) created by ultrasonic transducer which converts high-frequency electrical signal into high-frequency linear mechanical motion (or vibration). These vibrations are transmitted to the tool via mechanical amplifier. The tool and tool holder are designed to vibrate at their resonance frequency so that the maximum material removal rate (MRR) can be achieved.

The individual abrasive grains that come into contact with the vibrating tool acquire high velocity and are propelled towards the work surface. High-velocity bombardment of the work surface by the abrasive particles gives rise to the formation of a multitude of tiny highly stressed regions, leading to cracking and fracture of the work surface, resulting into material removal. The magnitude of the induced stress into the work surface is proportional to the kinetic energy ($1/2\,mv^2$; m = particle mass, v = particle velocity) of the particles hitting the work surface. Thus, a brittle material can be more easily machined than a ductile material. As the material is removed from the work surface, the gap between the tool bottom face and the work surface being machined increases, hence the machining efficiency goes down. To maintain the high efficiency of USM, the tool is constantly fed towards the workpiece such that the surface recession rate (or linear material removal rate – MRR_l) is equal to the tool feed rate (f).

The size of the cavity produced during USM is slightly larger than the tool dimensions (or tapered, Figure 11.3). A cylindrical solid tool of diameter D produces a circular hole of diameter $D + \Delta D$, where ΔD depends upon various process parameters and the location where it is being measured. The drilled hole also has a small taper (angle θ). The value of taper angle can be reduced by giving a reverse taper on the tool.

Ultrasonic machining machines are available in the power output range of 40 W to 2.4 kW. These machines usually have five sub-systems, namely, power supply, transducer, tool holder, tool and tool feed system, and slurry and slurry supply system.

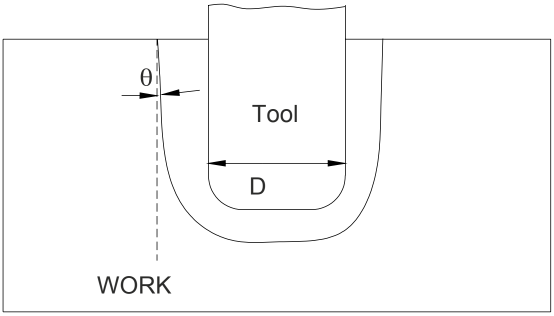

Figure 11.3. Tapered hole produced by USM (θ is the taper angle)

A high-power sine wave generator converts low-frequency (60 Hz) electrical power to high-frequency ($\approx$20 kHz) electrical power. This high-frequency electrical signal is transmitted to the transducer, which converts it into high-frequency low-amplitude vibration. In USM, either of two types of transducers are used, *i.e.*, piezoelectric (for low powers up to 900 W) or magneto-strictive type (for high powers up to 2.4 kW). Magneto-strictive transducers are made of nickel or nickel alloy sheets and their efficiency (20–35%) is much lower than the piezoelectric transducers' efficiency (up to 95%), hence cooling is essential in the case of magneto-strictive transducer to remove waste heat. The maximum change in length (or amplitude of vibration) that can be usually achieved is 25 μm.

The tool holder holds and connects the tool to the transducer (Figure 11.2), transmits the energy and, in some cases, amplifies the amplitude of vibration. Amplifying tool holders give as much as six times increased tool motion, and yield an MRR up to ten times higher than non-amplifying tool holders. The material of the tool should therefore have good acoustic properties, and high resistance to fatigue cracking. Commonly used materials for the tool holder are Monel (for low-amplitude applications), titanium and stainless steel. Tools are usually made of relatively ductile materials (brass, stainless steel, mild steel, *etc.*) to minimize tool wear rate (TWR). The ratio of TWR and MRR depends upon the type of abrasive, workpiece material and the tool material. The surface finish of the tool affects the surface finish obtained on the workpiece.

Hardness, particle size, usable life time and cost are used as criteria for selecting abrasive grains for USM. Commonly used abrasives (in order of increasing hardness are Al_2O_3, SiC and boron carbide (B_4C). Abrasive hardness should be greater than the hardness of the workpiece material. The MRR and surface finish obtained during USM also depend on the size of the abrasive particles. Fine grains result in a low MRR and good surface finish while the reverse is true with coarse grains. The mesh size of commonly used grits range from 240 to 800. Abrasive slurry consists of water and abrasives usually in the ratio 1:1 (by weight). However, this can vary depending upon the type of operation. Thinner (or lower-concentration) mixtures are used while drilling deep holes, or machining complex cavities so that the slurry flow is more efficient. The slurry, which is stored in a reservoir, is pumped to the gap formed between the tool and the work.

11.2.1.1 Process Parameters, Capabilities and Applications

USM process performance depends on the abrasive (material, size, shape and concentration), the tool and tool holder (tool material, frequency of vibration and amplitude of vibration) the and workpiece material (hardness). An increase in the amplitude of vibration increases the linear material removal rate (MRR_l) for different pressures (Figure 11.4). An increase in grit size also increases MRR_l but exhibits an optimum value (Figure 11.5). However, increase in MRR_l also results in higher value of surface roughness (R_a) (or poorer surface finish). As the cutting depth increases, the flow of slurry through the cutting zone becomes inefficient, hence MRR_l decreases further. Materials that can be easily machined by this process include ceramics, glass, carbides, *etc*., which cannot be efficiently machined by traditional methods. It is also quite useful for electrically non-conductive ceramics and fragile components. It can drill multiple holes at a time. Following are some of the capabilities of this process:

- Aspect ratio (ratio of hole length to diameter): 40:1
- Hole depth: 51–152 mm (with special flushing arrangement)
- MRR_l: 0.025–25 mm/min
- Surface finish: 0.25–0.75 μm
- Surface texture: non-directional
- Accuracy or radial overcut: 1.5–4.0 times the mean abrasive grain size

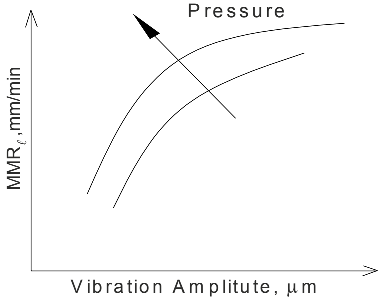

Figure 11.4. Effect of amplitude of vibration on penetration rate (MRR_l) for different pressures

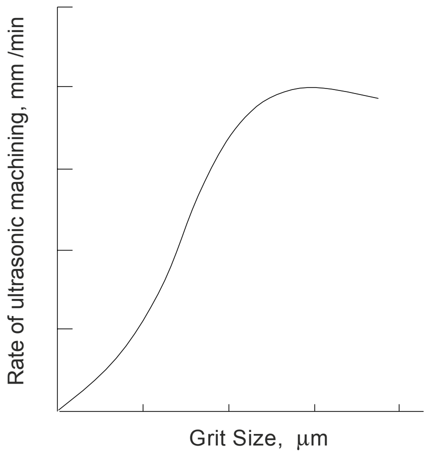

Figure 11.5. Effect of amplitude of vibration on penetration rate (MRR_l) for different pressures

11.2.2 Abrasive Water Jet Cutting (AWJC)

The abrasive water jet cutting (AWJC) process is a high-potential process applicable to both metals as well as non-metals. In this process, a high-velocity

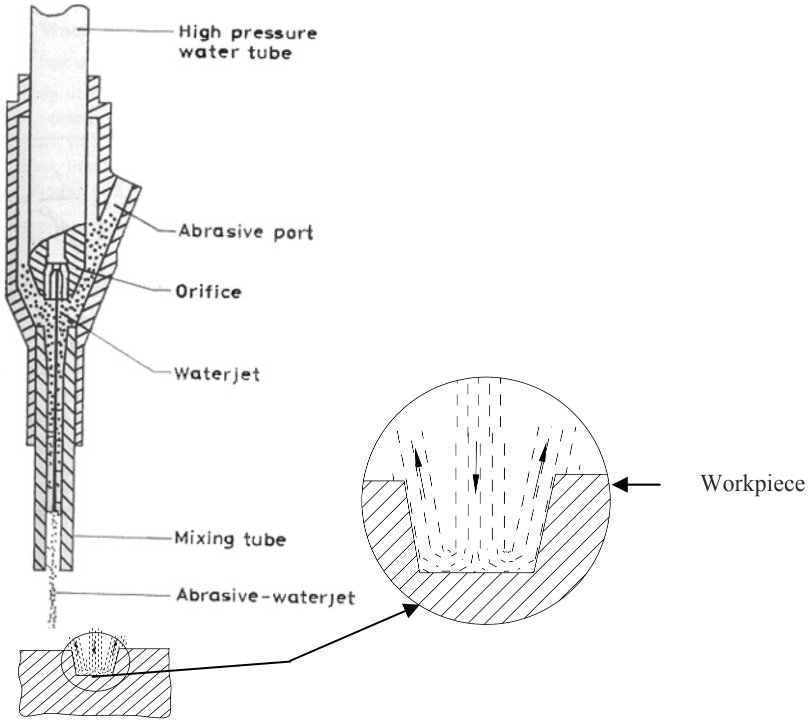

Figure 11.6. Details of abrasive water jet nozzle

water jet mixed with fine abrasive particles hits the workpiece surface (Figure 11.6). The velocity of the abrasive mixed water jet is very high, hence the kinetic energy with which the abrasive particles and the water jet hit the workpiece surface is very high (as high as 900 m/s in special cases) and hence it leads to the erosion of the work surface. Here, a part of the momentum of water jet is transferred to the abrasives, hence the velocity of abrasives rises rapidly.

Depending upon the type of the workpiece material being cut and the depth at which cutting is taking place, material removal occurs due to erosion, shear or failure under a rapidly changing localized stress field. The pressure at which a water jet operates is about 400 MPa, which is sufficient to produce a jet velocity of 900 m/s. Such a high-velocity jet is able to cut materials such as ceramics, composites, rocks, metals *etc*. [6]. Material removal by erosion takes place in the upper part of the workpiece while it occurs by deformation wear at the lower part of the workpiece being cut. The AWJC process can easily cut both electrically non-conductive and conductive, and difficult-to-machine materials. This process does not produce dust, thermal defects, and fire hazards. Recycling of water and abrasives is possible to some extent. It is a good process for shaping and cutting of composite materials, and creates almost no delamination.

11.2.2.1 AWJC Machine

Abrasive water jet cutting machines have four basic elements: a pumping system, abrasive feed system, abrasive water jet nozzle and catcher. The pumping system produces a high-velocity water jet by pressurizing water up to as high as 400 MPa using a high-power motor. The water flow rate can be as high as 3 gallons per minute. To mix the abrasives into this high-velocity water jet, the abrasive feed system supplies a controlled quantity of abrasives through a port. The abrasive water jet nozzle mixes abrasives and water (in mixing tube) and forms a high-velocity water abrasive jet. Sapphire, tungsten carbide, or boron carbide can be used as the nozzle material. There are various kinds of water abrasive jet nozzles. Another element of the system is a catcher, for which two configurations are commonly known: a long narrow tube placed under the cutting point to capture the used jet with the help of obstructions placed alternately in the opposite direction and a deep water-filled settling tank placed directly underneath the workpiece in which the abrasive water jet dies out.

11.2.2.2 Process Parameters, Capabilities and Applications

Independent process parameters include water (pressure, flow rate), abrasive (type, size, flow rate), nozzle, traverse rate, the stand-off distance and workpiece material. For a specified workpiece material and process parameters, there is a minimum pressure (*i.e.*, critical pressure or threshold pressure) below which no cutting will take place [6]. The machined depth increases as the pressure increases, and this relationship becomes steeper as the abrasive flow rate increases. An increase in abrasive flow rate increases the machined depth, but beyond the critical value of abrasive flow rate the machined depth starts to decrease. Various types of abrasive particles can be used during AWJC, *viz*. Al_2O_3, SiC, silica sand, garnet sand, *etc*. It is also found that, with an increase in traverse rate (relative motion between the water abrasive jet and workpiece) and stand-off distance (the distance between the nozzle tip and the workpiece surface being cut) the machined depth decreases. Under certain circumstances, more than one pass of cutting may be required, in which case less power is consumed compared with single-pass cutting. A theoretical model has also been proposed [7] to predict the penetration of an abrasive jet in a piercing operation.

The capabilities and specification of AWJC process are:

- Pressure : Up to 415 MPa
- Jet velocity : Up to 900 m/s
- Abrasive : Al_2O_3. SiC, silica sand
- Abrasive mesh size : 60 – 300
- Nozzle material : Sapphire, WC, B_4C
- Water requirement : Up to 3 gallons/min

This process has been applied to cut both metals as well as non-metals. AWJC process is good to cut honeycomb material, corrugated structures, *etc*. This process is gaining acceptability as a standard cutting tool in industries such as aerospace, nuclear, oil, foundry, automotive, construction *etc*.

11.3 Thermoelectric Advanced Machining Processes

Application of AMP is quite common in making holes in difficult-to-machine materials as well as shaping and sizing a part. Sometimes holes with a high aspect ratio or a large number of holes in a workpiece without burrs and without residual stresses are needed. Some processes are good only for electrically conductive materials while others are excellent for making thousands of holes in a square centimetre area of metallic as well as non-metallic materials. Processes such as EDM, travelling-wire EDM, LBM and EBM fall into the category of thermal AMP in which material removal takes place by melting or melting and vaporization. The energy source for material removal is in the form of heat.

In this section only two thermoelectric processes are discussed: electrical discharge machining (EDM), including travelling-wire EDM (TW-EDM), and laser beam machining (LBM).

11.3.1 Electric Discharge Machining (EDM) and Wire EDM

The working principle of EDM process can be understood from Figure 11.7(a). Dielectric flows through the gap between the electrodes (usually with the tool as the cathode and the workpiece as the anode), which are connected to a pulsed direct-current (DC) power supply. This produces sparks between the electrodes, which melt and sometimes vaporize material from both the tool and the workpiece. To improve the accuracy of axisymmetric profiles, orbital EDM is advocated. Figure 11.7(a) shows an inter-electrode gap between the tool and the workpiece in which dielectric is flushed at high pressure. As shown in Figure 11.7(b), once the power supply is on, the capacitor keeps charging until the breakdown voltage (V_b) is attained and then sparking takes place at a point of least electrical resistance. After each discharge, the capacitor recharges (Figure 11.7(b)) and the spark energy is shared mainly by workpiece, tool, dielectric and debris (removed material). Radiation losses are also present. The flowing dielectric in the IEG cools the tool and workpiece, cleans the IEG and localizes the spark energy into a small cross-sectional area.

The spark radius is usually very small (100–200 μm) [8] however the spark energy density is very high, hence the electrode's material melts and vaporizes in the localized area. The craters formed in this way spread over the entire surface of the workpiece under the tool. The cavity produced in the workpiece is approximately the replica of the tool. However, tool wear should be minimized by selecting optimum machining parameters and appropriate polarity. The material eroded from the electrodes is known as debris, which is a mixture of irregularly shaped particles and spherical particles. A very small gap (usually ≤ 100 μm) between the two electrodes is maintained with the help of a servo system. Figure 11.7(c) shows a photograph of an EDM m/c. It shows various important elements of an EDM m/c.

An allied EDM process has been developed, known as travelling-wire EDM (TW-EDM). In travelling-wire EDM, in place of a solid tool, a wire is used as the cathode (Figure 11.7(d)). The wire travels through the workpiece in its axial direction while the workpiece is fed in the *X* and *Y* directions to give it different shapes. The TW-EDM system is computer controlled and it can machine complicated 3D shapes.

(a)

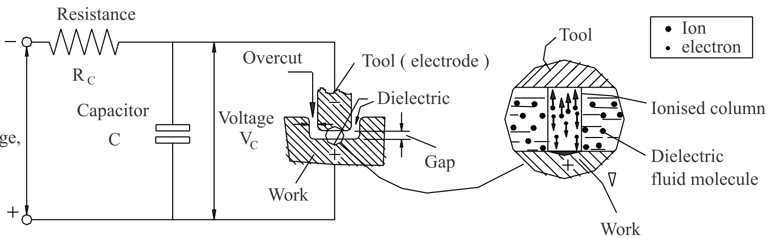
Resistance
R_C
D.C.
Supply Voltage,
V_S
Capacitor
C
Voltage
V_C
Overcut
Tool (electrode)
Dielectric
Gap
Work
Tool
Ion
electron
Ionised column
Dielectric
fluid molecule
Work

(b)

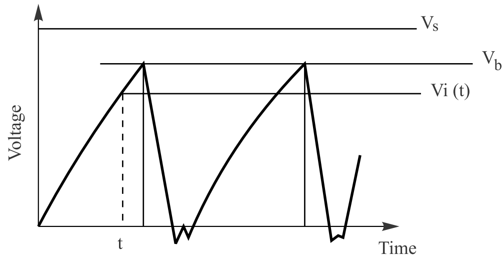
V_S
V_b
Vi (t)
Voltage
t
Time

(i)


Current
Time

(ii)

(c)

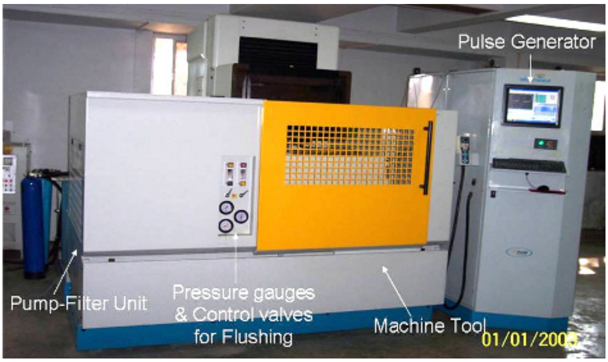
Pulse Generator
Pump-Filter Unit
Pressure gauges
& Control valves
for Flushing
Machine Tool

(d)

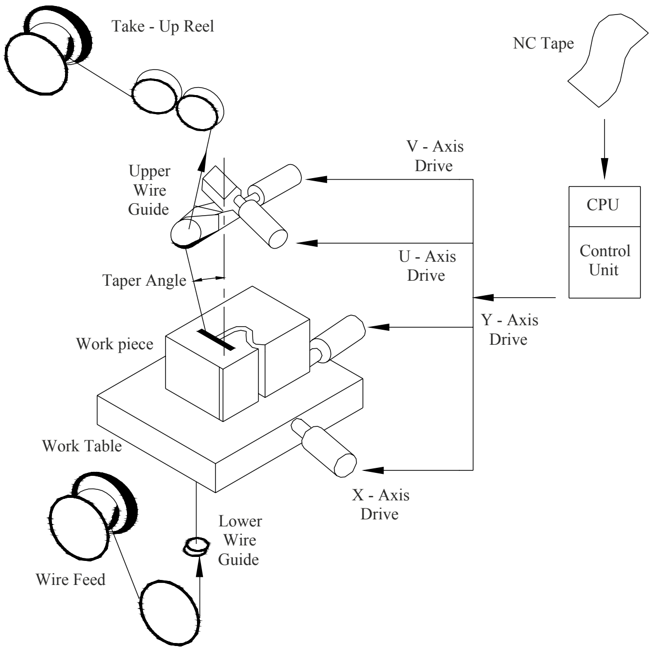

Figure 11.7. (a) Electric discharge machining using relaxation circuit **(b)** (i) Voltage versus time relationship, (ii) Current versus time relationship in EDM using relaxation circuit. V_s = supply voltage, V_b = breakdown voltage, V_i = instantaneous voltage **(c)** EDM machine (Courtesy: Electronica Machine Tools Limited, Pune, India) **(d)** Schematic illustration of travelling wire electric discharge machining process

Usually, 80–100 V DC pulses at approximately 5 kHz are passed through the electrodes. Negatively charged particles (electrons) break loose from the cathode surface under the influence of electric field forces. These electrons collide with the neutral molecules of the dielectric (kerosene, oil, or water) and produce electrons and ions, resulting in further ionization. In this ionized narrow channel, there is a continuous flow of a considerable number of electrons towards the anode and of ions towards the cathode. When these particles hit the electrodes their kinetic energy (KE) is converted into heat energy due to the bombardment of electrons onto the anode and ions on the cathode. Finally, localized high temperature at the electrodes results in the melting and/or vaporization of electrodes. Usually, a component made by EDM is machined in two stages, *viz.* rough machining (high MRR and high Ra value) and finish machining (low MRR and low Ra value).

The power supply of an EDM process should be able to control the parameters of voltage, current, duration and frequency of a pulse, and duty cycle (the ratio of on-time to pulse time). Figure 11.8 shows the on-time, off-time, pulse time and duty cycle for an ideal pulse. Also, the filtration of dielectric fluid before re-circulation is essential so that changes in its properties are minimal during the process. Effective flushing of dielectric is an important parameter and it removes by-products from the gap. Various methods of flushing are shown in Figure 11.9.

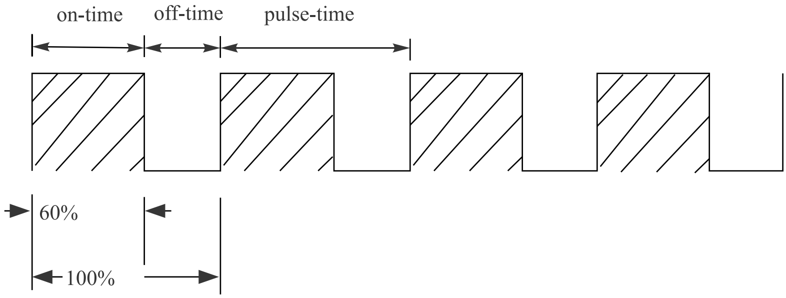

Figure 11.8. An illustration of on-time, off-time, pulse time and duty cycle

An increase in current results in an increase in MRR as well as an increased value of surface roughness, as shown in Figures 11.10(a,b). However, an increase in spark frequency results in an improved surface finish through a lower Ra value, as shown in Figure 11.10(c).

In TW-EDM, to minimize frequent breakage of wire and its rethreading at high load, stratified wire (copper core with zinc clad) is used (Figure 11.11); it also has the advantage of not being too expensive. One can easily obtain a surface finish of the order of 0.1 μm using TW-EDM. Nowadays, CNC-EDM and CNC-TW-EDM machines are equipped with an automatic tool changer, automatic wire feeder, automatic workpiece changer, automatic pallet changer and automatic position compensator. With the adoption of such functions in EDM, flexible manufacturing cells (FMC) are under design consideration [9].

To enhance the capabilities of EDM process, hybrid EDM processes have been developed. For example, electric discharge diamond grinding (EDDG → EDM + grinding) [10] and ultrasonic-assisted EDM [11] are two such hybrid EDM processes. EDDG of very hard materials such as WC is advantageous because electric discharges thermally soften work material, thus facilitating grinding. Continuous in-process dressing of grinding wheel gives stable grinding performance [1]. It is observed that specific energy in EDDG decreases with increasing pulse current.

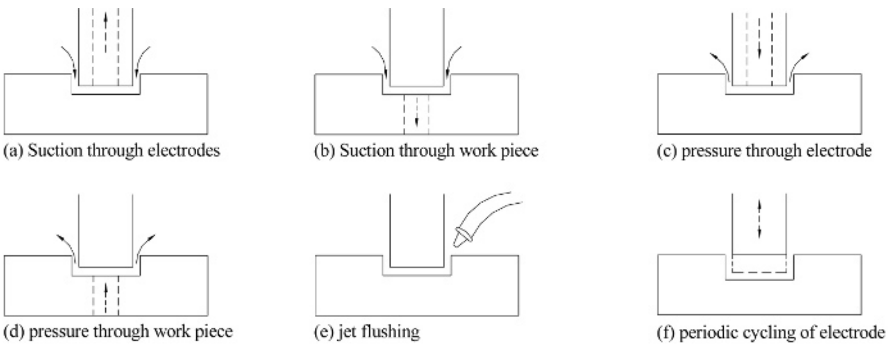

Figure 11.9. Various methods for dielectric flushing: **(a)** suction through electrode **(b)** suction through workpiece, **(c)** pressure through velectrode, **(d)** pressure through workpiece, **(e)** jet flushing, **(f)** periodic cycling of electrode [Courtesy: HMT, Bangalore, India]

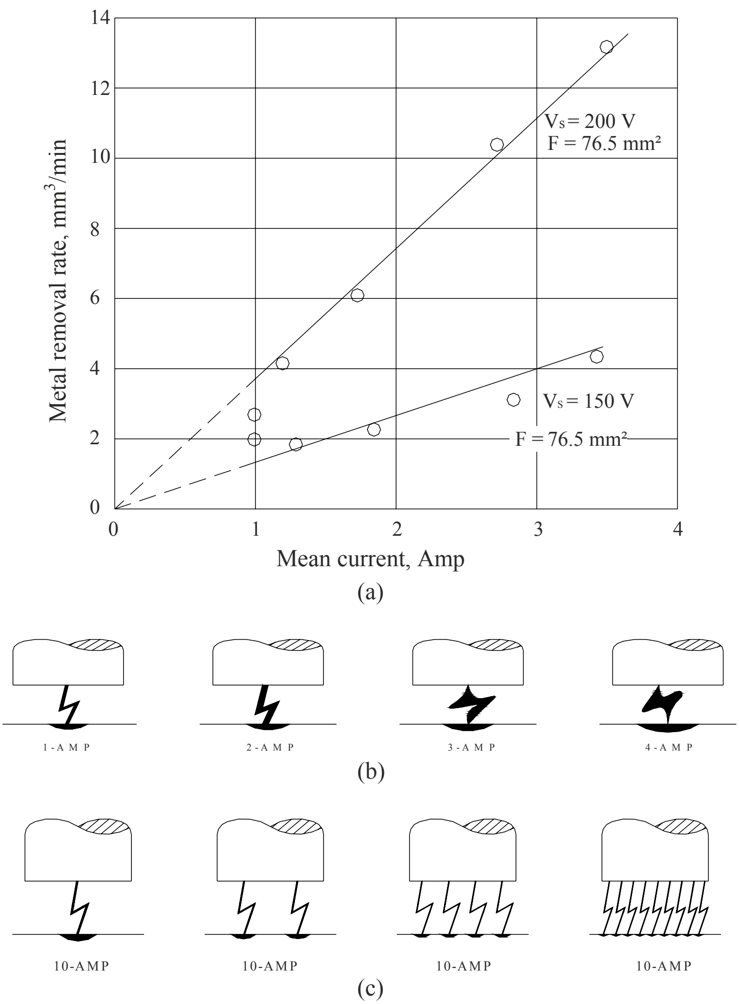

Figure 11.10. (a) Effect of mean current on MRR for different voltages. Dielectric = kerosene, tool = brass, work material = low carbon steel, F = Tool Electrode Area [12]. **(b)** Effect of current on surface finish (or crater size). **(c)** Effect of frequency of sparking on surface finish (or crater size)

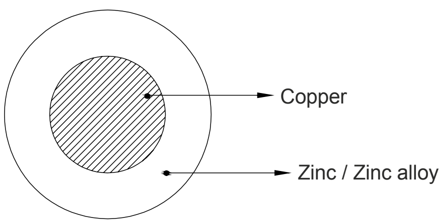

Figure 11.11. Stratified wire used in TW-EDM

11.3.1.1 Process Capabilities and Applications

EDM can be used only for electrically conductive materials, and its performance is not substantially affected by mechanical, physical and metallurgical properties of workpiece material. It can perform various kinds of operations such as drilling, cutting, 3D shaping and sizing (wire EDM) and spark-assisted grinding (EDDG). It gives good repeatability and accuracy of the order of 25–125 μm. The tolerances that can be achieved are ±2.5 μm. This has been used to produce as good as 100:1 aspect ratio holes. Under normal conditions, the volumetric material removal rate (MRR_v) is in the range of 0.1–10 mm^3/min. The surface finish produced during EDM is usually in the range 0.8–3 μm, depending upon the machining conditions used. The machined surface normally has a recast layer which should be removed before fitting the part into the assembly or sub-assembly. It is commonly used for making hardened steel dies and moulds and has numerous applications in various types of industries.

11.3.2 Laser Beam Machining (LBM)

The acronym laser means light amplification by stimulated emission of radiation. In laser beam machining, a laser beam is focussed onto the target/workpiece surface (Figure 11.12(a)), resulting in an energy density of the order of 10^3 W/mm^2 (or more in some cases), which is enough to melt and vaporize materials such as diamond. Holes drilled using a laser beam system are normally not straight sided, as shown in Figure 11.12(b). Laser light is monochromatic, coherent and gives very low divergence. An LBM machine has high capital and operating costs, and very low machining efficiency (<1%). Industrial lasers operate either in continuous wave (CW) or in pulse mode [13]. CW lasers are used for processes such as

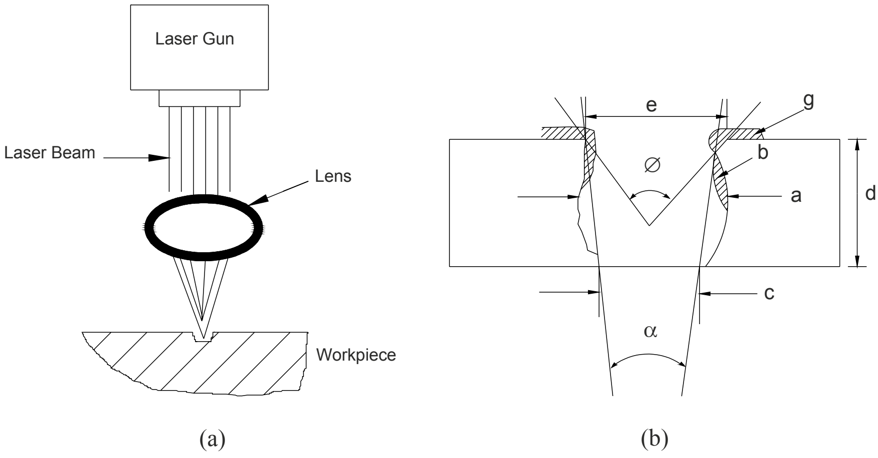

Figure 11.12. (a) Schematic diagram of laser beam machining (LBM). **(b)** Cross-section of a hole drilled by LBM: a – diameter of the mid span, b – thickness of the recast layer, c – exit diameter; d – hole depth, e – inlet diameter; g – thickness of the surface debris, ϕ - inlet cone angle, α - taper angle

welding, laser chemical vapour deposition (LCVD) and surface hardening. These applications require uninterrupted supply of energy for melting and phase transformation. Controlled pulse energy is desirable for processes such as cutting, drilling, marking *etc*., so that the heat-affected zone (HAZ) is minimal.

LBM is capable of machining refectory, brittle, hard, metallic and non-metallic materials. As long as the laser beam path is not obstructed, it can be used to machine in otherwise inaccessible areas. LBM is suitable for drilling very small-diameter holes with a reasonable large aspect ratio. LBM is used for drilling, trepanning, trimming, marking, welding and similar other operations. It is used for both micromachining as well as macromachining. LBM has also been used for 3D machining, namely, threading, turning, grooving *etc.* [13].

11.4 Electrochemical Advanced Machining Processes

11.4.1 Electrochemical Machining (ECM)

ECM works on the principle of Faraday's laws of electrolysis. The noteworthy feature of electrolysis is that electrical energy is used to produce a chemical reaction, therefore the machining process based on this principle is known as electrochemical machining (ECM). In ECM, a small DC potential (5–30 V) is applied across two electrodes (the workpiece being the anode and the tool the cathode). Electrolyte flows in the gap between these two electrodes (Figure 11.13). Transfer of electrons between ions and electrodes completes the electrical circuit. During the flow of current in the circuit, metal is detached atom by atom from the anode surface and appears in the electrolyte as ions (Fe^{2+}). These ions form the precipitate of metal hydroxides ($Fe(OH)_2$) (Figure 11.13). During the electrolysis of water, its molecules gain electrons from the cathode so that they separate into free hydrogen gas and hydroxyl ion as

$$H_2O + 2e^- \rightarrow H_2 \uparrow + 2OH^- .$$

As the anode dissolves, positively charged metal ions appear in the electrolyte, which combine with negatively charged hydroxyl ions to form metal hydroxides as

$$Fe - 2e^- \rightarrow Fe^{2+}$$

$$Fe^{2+} + 2OH^- \rightarrow Fe(OH)_2 .$$

These hydroxides are insoluble in water hence they appear as a precipitate and do not affect the chemical reaction. Ferrous hydroxides may further react with water and oxygen to form ferric hydroxides.

$$Fe(OH)_2 + 2H_2O + O_2 \rightarrow 4Fe(OH)_3 .$$

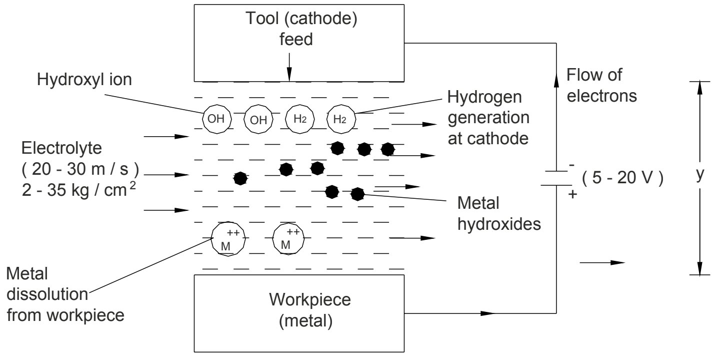

Figure 11.13. Schematic diagram of electrochemical machining

During ECM, metal from the anode is removed atom by atom by removing negative electrical charge that binds the surface atoms to their neighbours. The ionized atoms (say, Fe^{2+}) are attracted away from the workpiece by an electric field. The rate of removal of Fe^{2+} from the anode is governed by Faraday's laws of electrolysis. The amount of chemical change m (the substance deposited or dissolved) is proportional to the amount of charge passed through the electrolyte. The amount of change produced (substances deposited or dissolved) by the same quantity of charge is proportional to the chemical equivalent weights of the material. These laws can be expressed as follows:

$$m \propto I\, t$$

and

$$m \propto E$$

Therefore,

$$m = \frac{ItE}{F} = \frac{AIt}{Z.F} \tag{11.1}$$

where I is the current (A), t is the time (s), E is the gram-equivalent weight of material (or A/Z, where A is gram atomic weight and Z is the valency of dissolution), F is Faraday's constant (96500 As), and m is mass of the metal dissolved/deposited (g). Dividing both sides of the above equation by time t will give MRR_g (the material removal rate in units of g/s) as

$$MRR_g = \frac{m}{t} = \dot{m} = \frac{IE}{F}. \tag{11.2}$$

To obtain the volumetric material removal rate MRR_v, divide both sides of Equation (11.2) by the density of the metal (or alloy) as

$$MRR_v = \frac{MRR_g}{\rho_a} = \frac{IE}{\rho_a F} \tag{11.3}$$

This equation can be used to calculate the linear material removal rate MRR_l by dividing it by cross sectional area (A_r) of the tool (or smaller electrode):

$$MRR_l = \frac{IE}{\rho_a A_r F} \tag{11.4}$$

The accurate evaluation of m from Equation (1) is difficult when the anode is an alloy because the value of E for the alloy is not known. It can be evaluated either by the percent-by-weight method or the superposition-of-charge method. Furthermore, many elements have more than one valency of dissolution. The exact valency of dissolution under the given machining conditions should be known because $E = A/Z$. The current I is the function of applied voltage (V), interelectrode gap (IEG) and electrolyte conductivity (k). The gap between the bottom surface of the tool and the top dissolving surface of the workpiece is known as the inter-electrode gap (IEG), abbreviated as y. The smaller the IEG, the greater the current flow (or current density) will be. Furthermore, MRR_g depends on the current efficiency (η), which usually varies between 75% and 100%. Theoretically, the MRR depends upon the current passing through the workpiece and its chemical composition. To maintain a constant gap (or equilibrium gap), the tool should be fed towards the workpiece at the rate (f) at which the workpiece surface is recessing downwards (MRR_l). Hence,

$$f = MRR_l \tag{11.5}$$

11.4.2 ECM Machine

An ECM machine tool consists of four main subsystems: the power source, the electrolyte cleaning and supply system, the tool and tool feed system and the work and work holding system. The power source supplies a low-voltage (5–30 V) high-current (as high as 40 kA) rectified DC power supply. Figure 11.14 shows a photograph of a simple low-capacity ECM machine.

The electrolyte supply and cleaning system consists of a pump, filters, piping, control valves, heating/cooling coils, pressure gauge and a tank/reservoir. These elements should be made of anti-corrosive materials because the electrolyte used is corrosive in nature. Tools are also required to operate in a corrosive environment for a long period of time. Hence, they should also be made of anti-corrosive material having high thermal and electrical conductivity, and easy-to-machine characteristics (high machinability). Copper, brass and stainless steel are commonly used materials for making ECM tools. It is important to know that only electrically conductive materials can be machined by this process. However, work holding devices are made of electrically non-conducting materials having good thermal stability, corrosive resistance and low moisture absorption. Glass-fibre-reinforced plastics (GFRP), Perspex and plastics are some such materials that can be used to fabricate work holding devices.

To exploit the full potential of the process, many allied processes/operations have been developed using the principle of anodic dissolution described above.

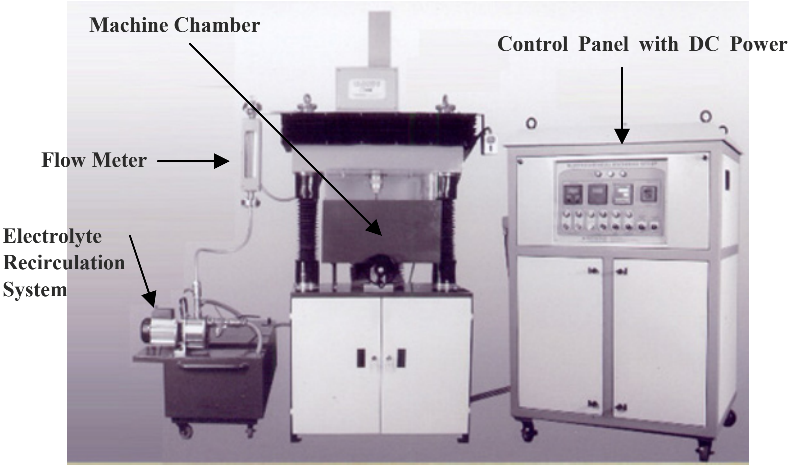

Figure 11.14. ECM machine (Courtesy: Metatech Industries, Pune, India)

Some of the allied ECM operations are electro-chemical boring, electro-chemical broaching, electro-chemical ballizing, electro-chemical drilling, electro-chemical deburring, electro-chemical die sinking, electro-chemical milling, electro-chemical sawing, electro-chemical micromachining, electro-chemical turning, electro-chemical trepanning, electro-chemical wire cutting, electro-stream drilling and shaped tube electromachining (STEM) [1]. Shaped tube electro-chemical drilling (STED) has been successfully used to drill small-diameter high-aspect-ratio holes in difficult to machine materials such as nimonic alloys (Figure 11.15) [14].

To enhance the capabilities of the base process (here ECM), two or more processes are combined together to make it a hybrid process. Some of these hybrid processes are electro-chemical grinding (ECG) [15], electro-chemical honing (ECH) [16], and electro-chemical spark machining [17–22]. Such hybrid processes give better performance than the constituent processes (ECM + grinding, or ECM + honing or ECM + EDM).

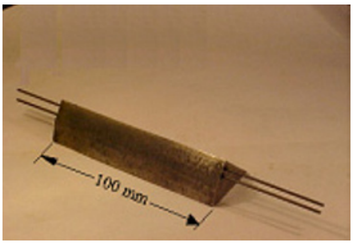

Figure 11.15. Photograph of a nimonic super alloy part in which a 100-mm-deep hole has been drilled using the STED process [14]

11.5 Fine Finishing Processes

11.5.1 Abrasive Flow Machining (AFM)

With today's focus on total automation in the flexible manufacturing systems, the abrasive flow machining (AFM) process offers both automation and flexibility. This process was developed basically to deburr, polish and radius difficult-to- reach surfaces and edges by flowing abrasive laden polymer, to and fro in two vertically opposed cylinders (Figure 11.16(a)) [23, 24]. The medium (a mixture of

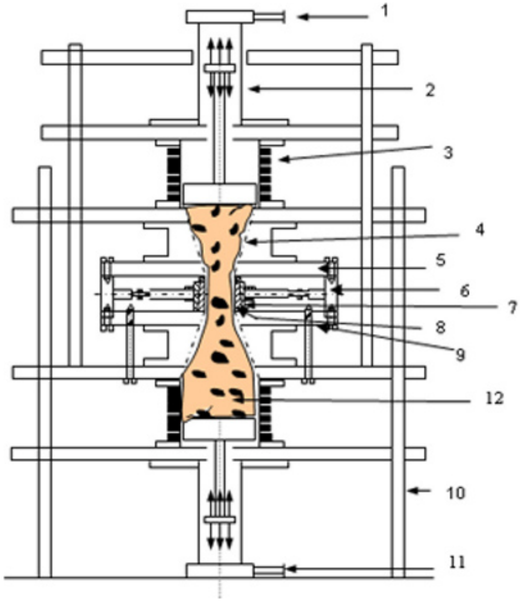

(a)

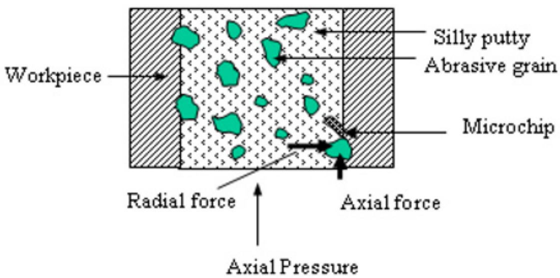

(b)

Figure 11.16. (a) Schematic diagram of abrasive flow machining setup: 1 – hydraulic oil inlet/outlet port, 2 – hydraulic cylinder, 3 - medium cylinder, 4 – smooth entry profile, 5 – Top cover plate, 6 – dynamometer for force measurement, 7 – central hub, 8 – split cylindrical fixture with workpiece, 9 – botSstom cover plate, 10 – support frame, 11 – hydraulic oil outlet/inlet port, 12 – medium with abrasive particles. **(b)** Types of forces acting on a grain [23]

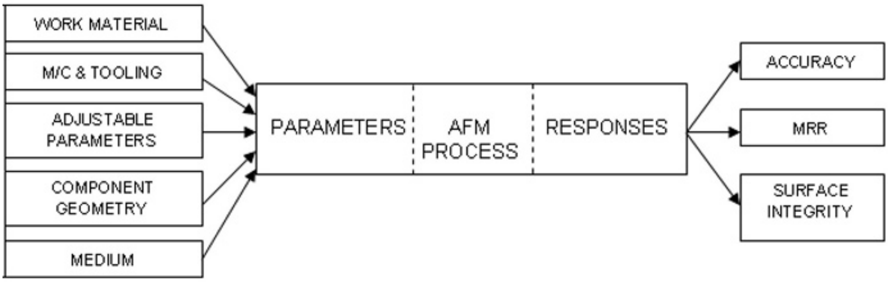

Figure 11.17. Variables and responses of AFM process

visco-elastic material, say, polyborosiloxane, additives and abrasive particles) enters the workpiece through the tooling. The abrasive particles (SiC, Al_2O_3, CBN, diamond) penetrate the workpiece surface depending upon the extent of the radial force

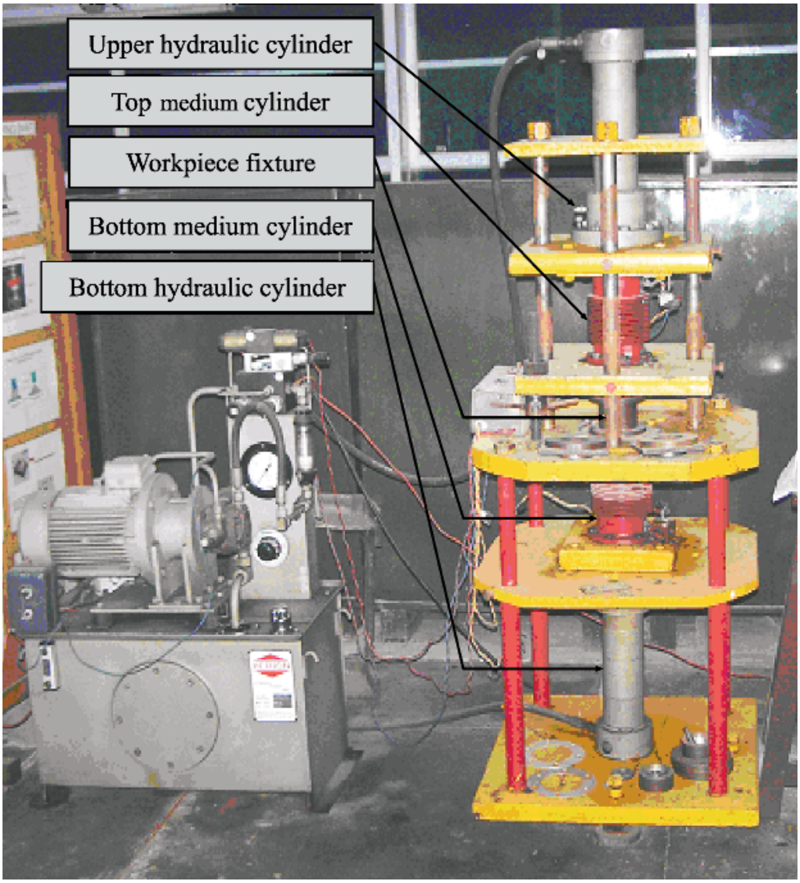

Figure 11.18. Experimental AFM setup [I.I.T. Kanpur]

acting on them. Due to the tangential/axial force, the material is removed in the form of microchips as shown in Figure 11.16(b). The medium is recirculated until the concentration of foreign particles increases to a level such that its finishing rate decreases substantially. At this time part of the used medium (say, 20%) is replaced by fresh medium. Figure 11.17 shows the variables and responses of the AFM process.

There are three major elements of the AFM system: the tooling, the machine, and the medium. Figure 11.18 shows a photograph of an AFM machine developed at IIT Kanpur for research and development activity. The tooling confines and directs the medium flow to the areas where abrasion is desired. The machine controls the extrusion pressure, which controls the medium flow rate. The abrasive-laden polymer is the medium, whose rheological properties determine the pattern and aggressiveness of the abrasive action. The rheological properties of the medium change during the AFM process and they substantially influence the process performance [25]. This process can be applied for finishing multiple pieces of the same shape and size (Fig-

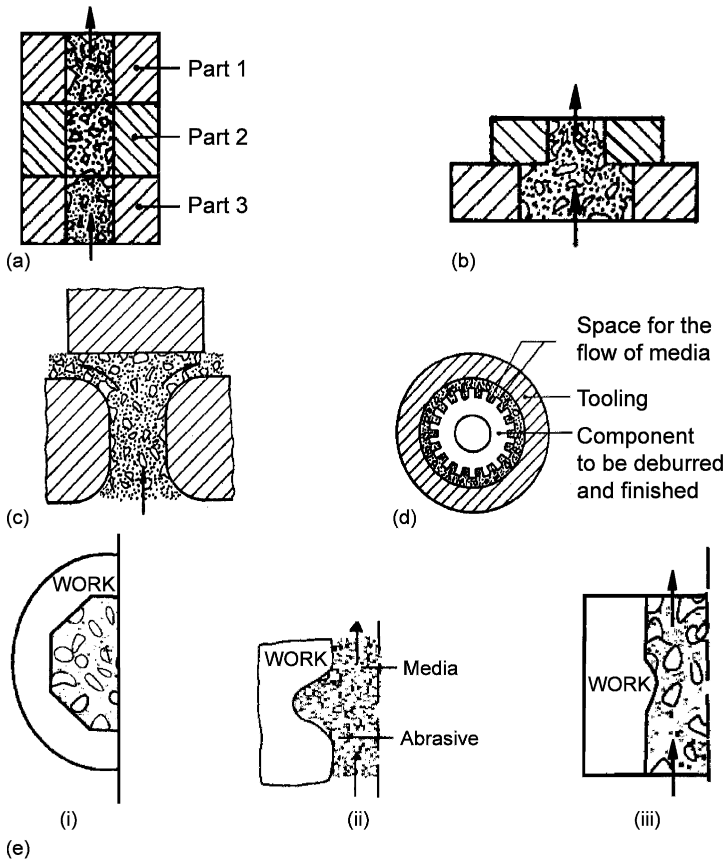

Figure 11.19. (a) Finishing of multiple parts having the same configuration. **(b)** Finishing of two parts but with different configurations. **(c)** Finishing and radiusing of an internal hole. **(d)** Tool for deburring and finishing of a gear using the AFM process. **(e)** medium acting as a self-deformable stone in the case of a complex, convex and concave component [1]

ure 11.19(a)), and also of different size (Figure 11.19(b)). It can radius the edges of a part (Figure 11.19(c)) and can finish a complete gear in one go (Figure 11.19(d)). The medium acts as a *self-deformable stone* and can finish concave, convex as well as complex-shaped components (Figure 11.19(e)). It also has some peculiar applications as well where no other traditional and advanced finishing processes can work. For example, a large number of small-diameter holes (say, diameter 3 mm and depth 30 mm) can be easily and simultaneously finished by this process, which is otherwise very difficult. This process can be used to control the surface finish of the cooling holes in a turbine blade, or the surface finish of stator and rotor blades of a turbine. The best surface finish achieved by this process is 50 nm.

11.5.2 Magnetic Abrasive Finishing (MAF)

In the magnetic abrasive finishing (MAF) process, granular magnetic abrasive particles (MAPs) [sintered ferromagnetic (iron) particles and abrasive grains (say, Al_2O_3, SiC, or diamond)] are used as cutting tools and the necessary finishing pressure is applied by an electromagnet-generated magnetic field. Figure 11.20(a) shows the working principle of the MAF process through a schematic diagram.

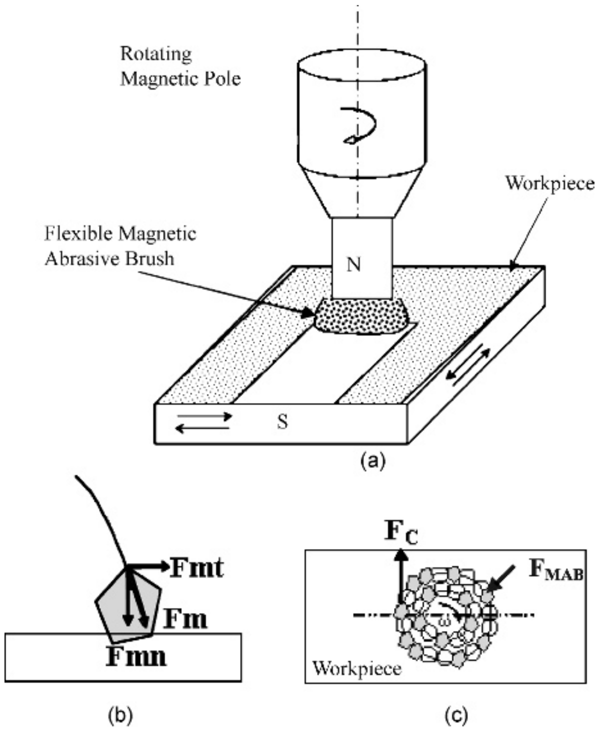

Figure 11.20. (a) Plane magnetic abrasive finishing of magnetic work material. **(b)** Schematic diagram showing the normal (F_{mn}) and tangential components (F_{mt}) of the magnetic force (F_m) acting on a magnetic abrasive particle. **(c)** FMAB and the cutting force (F_c) acting on an abrasive particle

The magnetic abrasive particles join each other magnetically between two magnetic poles (S and N) along the magnetic lines of force, forming a flexible magnetic abrasive brush (FMAB). When there is relative motion between the FMAB and the workpiece, abrasion takes place to give a polished finish. This finish can be as good as approaching to 50 nm, depending upon the machining conditions and workpiece material. The performance of the process depends on the parameters such as the MAP (type, size and mixing ratio), the working clearance (the gap between the workpiece surface being finished and the bottom face of magnetic pole), the rotational speed of the poles, the feed motion (x and y motion) of the workpiece, vibration (frequency and amplitude), the properties of the work material and the magnetic flux density [26–31].

Figure 11.20(b) shows the magnetic force (F_m) and its components: the magnetic normal force (F_{mn}) acting on a MAP due to the magnetic field, and the tangential force (F_c) acting mainly due to the rotation of the magnet (Figure 11.20(c)). There is a small contribution F_{mt} to this force F_c as a component of F_m (the magnetic force).

Figure 11.21(a) shows a schematic diagram of a magnetic abrasive finishing setup for plane surfaces. It shows the major elements of the setup, while Fig-

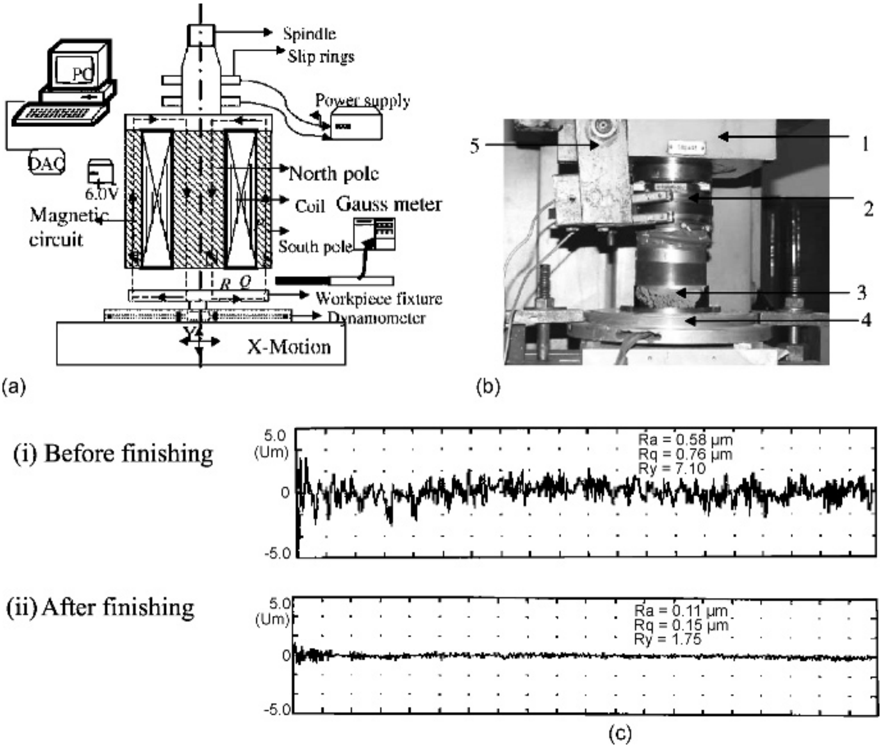

Figure 11.21. (a) Schematic diagram of plane magnetic abrasive finishing process setup. **(b)** Photograph of the plane MAF setup: 1 – column of a milling machine, 2 – slip ring, 3 – FMAB, 4 – ring dynamometer, 5 – slip ring attachment [28]. **(c)** Surface roughness plots (i) before, and (ii) after magnetic abrasive finishing of a stainless-steel workpiece

ure 11.21(b) shows a photograph of a part of a setup. Figure 11.21(c) shows the surface finish before (0.58 μm) and after (0.11 μm) MAF on a stainless-steel workpiece. This process can also be used to improve the surface properties by the process of diffusion of traces of MAP into the workpiece surface. Proper tooling can be developed to finish 3D intricate shapes because FMAB adapts to the shape of the workpiece, however it is not as flexible as the AFM medium.

Achieving uniform surface finish near the discontinuities or edges in the magnetic poles is difficult. At irregularities, the magnetic flux density is greater, hence the rate of change in surface roughness is also higher compared to other areas. There are various other areas in which research needs to be done, such as workpiece surface temperature and the forces acting on the workpiece during MAF processing. The effect of various parameters on responses such as MRR, surface roughness and out-of-roundness (in the case of cylindrical workpieces) have been reported [28, 29].

11.5.2.1 Internal Magnetic Abrasive Finishing

MAF can also be used for finishing internal surfaces. MAPs are blown with high pressure air jet. When the MAP jet comes into the domain of magnetic field, the particles slightly divert towards the source or pole of the magnetic field (the internal surface of the workpiece) and move forward due to an axial force (F_c), shearing the peaks off the internal surface. The path of the jet of the magnetic abrasive particles is slightly deviated due to the magnetic field force (F_m) (Figure 11.22) [32] so that the MAP flow abrades the internal surface of the tube. The velocity of

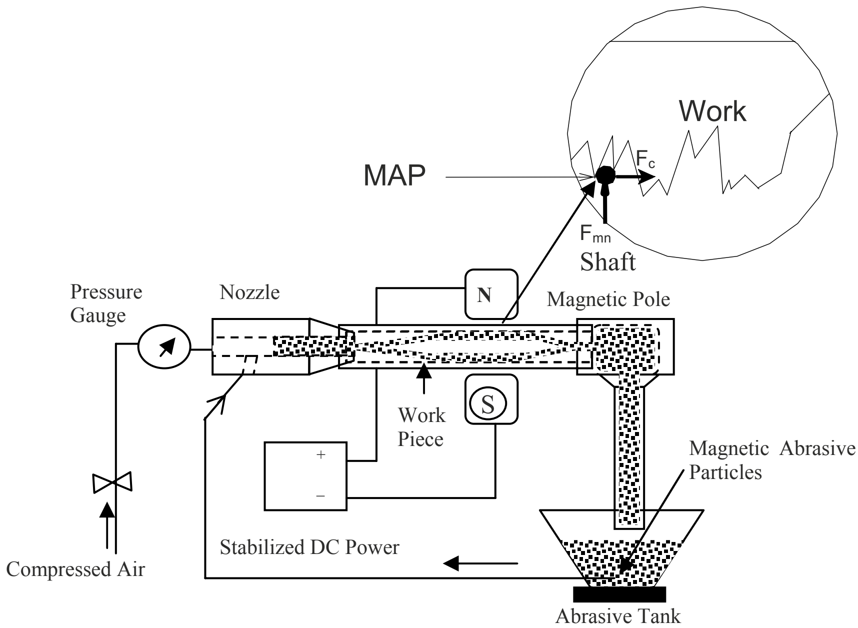

Figure 11.22. Magnetic abrasive jet finishing

the jet of MAPs is another important parameter of this process. However, this MAF technology needs to be brought out of the research laboratories so that it can be employed on the shop floor for industrial use. Results have been reported [26, 27] in the literature regarding finishing of stainless-steel rollers using MAF to obtain a final surface roughness R_a value of 7.6 nm from an initial surface roughness value of 220 nm.

11.5.3 Magnetic Float Polishing (MFP)

Various processes are available for finishing flat, complex-shaped and cylindrical surfaces but none of these processes qualifies for finishing spherically shaped workpieces, say, balls. A new process called magnetic float polishing (MFP) is applicable mainly for spherical balls. This process was developed for gentle finishing of very hard materials like ceramics, which develop defects during grinding, leading to fatigue failure. To achieve a low level of controlled forces, a magnetic field is used to support an abrasive slurry when finishing ceramic products, namely ceramic balls and rollers. This process is known as magnetic float polishing (MFP). This technique is based on the ferro-magnetic behaviour of the magnetic fluid that can levitate a non-magnetic float and suspended abrasive particles in it through the magnetic field. The levitation force applied by the abrasives is proportional to the magnetic field gradient and is extremely small and highly controllable. This is a good method for super-finishing of brittle materials with flat and spherical shapes [5, 27, 30, 31].

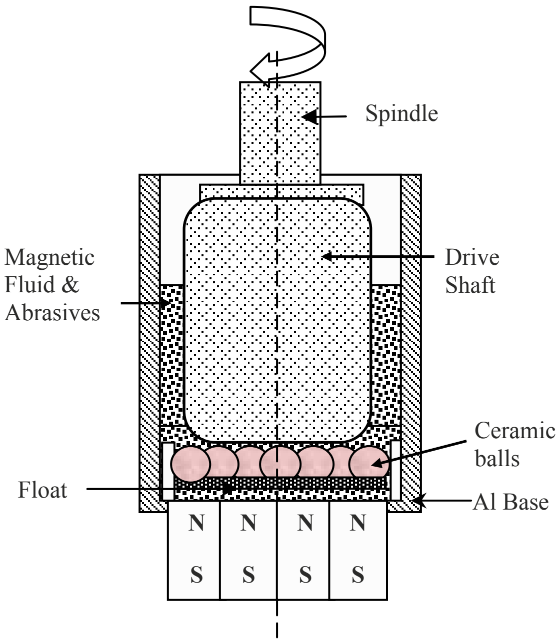

Figure 11.23. Schematic diagram of the magnetic float polishing apparatus

The setup consists of a magnetic fluid containing fine abrasive grains and extremely fine ferromagnetic particles in a carrier fluid (water or kerosene) (Figure 11.23). On the application of the magnetic field, the ferro-fluid is attracted downwards to the area of higher magnetic field. At the same time, a buoyancy force is exerted on the non-magnetic material, pushing it upward to the area of lower magnetic field. The abrasive grains, the ceramic balls, and the acrylic float inside the chamber, all being non-magnetic materials, are levitated by this magnetic buoyant force. The drive shaft is fed down to contact the balls and to press them down to reach the desired force level. The balls are polished by the relative motion between the balls and the abrasive particles.

11.6 Micromachining

Micromachining is sometimes misunderstood, as if it were performed only on microscale parts. Micromachining can be performed on both macro- and microcomponents. Micromachining encompasses all those processes in which material is removed at the micron level. Micromachining processes are classified mainly into two classes: bulk micromachining, where the objective is to shape and size a component, usually a miniaturized component; This also includes drilling/machining of microholes and microcavities. Here, material removal takes place in the micron domain (say, microchips), hence leading to the term *micromachining*. The second class includes surface micromachining, where the objective is to improve the surface finish to the micron or sub-micron (nanoscale) range. Surface roughness values obtained by some of these processes have been reported to be as low as the size of or a fraction of an atom. Table 11.1 shows the capabilities of some of the micro/nanofinishing processes. To be more precise, sub-micromachining and sub-microfinishing are also known as nanomachining and nanofinishing, respectively. The majority of AMPs are capable of performing nanomachining/nanofinishing operations.

Normally, mechanical-type advanced machining processes (MAMP) are used for macromachining, so their process parameters should be scaled down so they can be used for micromachining of both macro- and microproducts. For example, ultrasonic micromachining and abrasive water jet micromachining are two such processes. However, almost all advanced finishing processes (AFM, MAF, MRF, MRAFF, *etc.*) are microfinishing and nanofinishing processes. In these processes, material is removed in the form of chips of micron/nanosize. These processes are capable of producing a surface finish in the sub-micron range (Table 11.1). There is another class of processes, known as mechanical-type advanced finishing processes, in which material is removed in the form of atoms or molecules (such as elastic emission machining and ion beam machining). Such processes are capable of producing surface finish Ra values smaller than the size of an atom (Table 11.1), that is, in the sub-nano range.

In the case of thermal AMP, material is removed by melting and/or vaporization. Some of these processes have been modified to machine at the micro- or nanoscale. If EDM is performed with lower machining parameters it can easily be used for microdrilling or microshaping of miniature components. The same is true

Table 11.1. Surface finish obtainable from some advanced finishing processes

No.	Finishing process	Workpiece	Ra (nm)
1.	Grinding	–	25 – 6250
2.	Honing11	–	25 – 1500
3.	Lapping	–	13 – 750
4.	Abrasive flow machining (AFM) with SiC abrasives	Hardened steel	50
5.	Magnetic abrasive finishing (MAF) with diamond abrasives	Stainless steel rods	7.6
6.	Magnetic float polishing (MFP) with CeO_2 abrasives	Si_3N_4	4.0
7.	Magneto-rheological finishing (MRF) with CeO_2	Flat BK7 glass	0.8
8.	Elastic emission machining (EEM) with ZrO_2 abrasives	Silicon	<0.5
9.	Ion beam machining (IBM)	Cemented carbide	0.1

with laser beam micromachining. However, electron beam machining performs operations at the micro/nanolevel depending upon the values of the parameters selected. However, the use of PAC does not seem feasible for micromachining.

ECM is mainly used for bulk material removal specially for macrocomponents, however it has been appropriately scaled down for performing electro-chemical micromachining (ECMM) operations on both macro- and microproducts. Photochemical machining and chemo-mechanical polishing are already popular micromachining processes for macroproducts as well as for microproducts.

11.7 Finished Surface Characteristics

The performance of advanced fine abrasive finishing processes is evaluated by their achievable surface finish, form accuracy and resulting surface integrity. These fine abrasive finishing processes have been shown to yield accuracies in the nanometre range. The order of surface damage ranges from micrometres to nanometres in these advanced finishing processes. This makes their measurement a formidable task. Table 11.1 summarises the attainable surface finish of advanced fine finishing processes.

References

[1] Jain VK (2002) Advanced Machining Processes. Allied, New Delhi.
[2] Benedict GF (1987) Nontraditional Manufacturing Processes. Marcel Dekker, New York, NY.
[3] McGeough JA (1988) Advanced Methods of Machining. Chapman & Hall, London.

[4] McKeown PA (1987) The role of precision engineering in manufacturing of the future. Ann CIRP 36(2): 495–501.
[5] Taniguchi N (1983) Current status in, and future trends of, ultraprecision machining. Ann CIRP 32(2): 573–582.
[6] Hashish M (1989) A model for abrasive water jet (AWJ) machining. Trans ASME J Eng Mater Technol 111: 154–162.
[7] Hemanth P, Naqash PV, Ramesh Babu NR (2005) A simplified model for predicting the penetration of an abrasive water jet in a piercing operation. Int J Manuf Technol Manage 7(2–4): 366–380.
[8] Shankar P, Jain VK, Sundararajan T (1997) Analysis of spark profiles during EDM process. Mach Sci Technol 1(2): 195–217.
[9] Kobayashi K (1995) The present and future developments of EDM and ECM. Proc. XI ISEM, 29–47.
[10] Koshy P, Jain VK, Lal GK (1996) Mechanism of material removal in electric discharge diamond grinding. Int J Mach Tools Manuf 36(10): 1173–1185.
[11] Murthy VSR, Philip PK (1987) Pulse train analysis in ultrasonic assisted EDM. Int J Mach Tools Manuf 27(4): 469–477.
[12] Pandey PC and Shan HS (1980), Modern Machining Processes, published by Tata McGraw Hill, New Delhi.
[13] Chryssolouris G (1990) Laser Machining – Theory and Practice. Springer-Verlag, New York, NY.
[14] Bilgi DS, Jain VK, Shekhar R, Mehrotra S (2004) Electrochemical deep hole drilling in super alloy for turbine application. J Mater Proces Technol 149: 445–452.
[15] Gedam A, Noble CF (1971) An assessment of the influence of some wheel variables in peripheral electrochemical grinding. Int J Mach Tool Des Res 11: 1–12.
[16] Dubey AK, Jain NK, Shan HS (2006) Precision micro-finishing by electrochemical honing, Proceedings of ICOMAST 2006 held at Melaka, Malaysia.
[17] Adhikari S, Jain VK (2007) Some new observations in electrochemical spark machining (ECSM) of quartz. J Mater Process Technol doi: 01016/jmatprotec.2007.08.071.
[18] Gautam N, Jain VK (1998) Experimental investigations into ECSD process using various tool kinematics. Int J Mach Tools Manuf 38 (1–2): 15–27.
[19] Bhattacharyya B, Doloi BN, Sorkhel SK (1999) Experimental investigations into electrochemical discharge machining (ECDM) of non-conductive ceramic materials. J Mater Process Technol 95: 145–154.
[20] Jain VK, Chak SK (2000) Electrochemical spark trepanning of alumina and quartz. Mach Sci Technol 4:277–290.
[21] Jain VK, Dixit PM, Pandey PM (1999) On the analysis of the electrochemical spark machining process. Int J Mach Tools Manuf 39: 165–186.
[22] Jain VK, Rao PS, Choudhury SK, Rajurkar KP (1991) Experimental investigations into traveling wire electro-chemical spark machining (TW-ECSM) of composites. J Eng Ind 113: 75– 84.
[23] Gorana VK, Jain VK, Lal GK (2004) Experimental Investigation into cutting forces and active grain density during abrasive flow machining. Int J Mach Tools Manuf 44: 201–211.
[24] Gorana VK, Jain VK, Lal GK (2006) Prediction of surface roughness during abrasive flow machining. Int J Adv Manuf Technol 31(1/2): 258–267.
[25] Jain VK, Ranganatha C, Murlidhar K (2001) Evaluation of rheological properties of medium for AFM process. Mach Sci Technol 5(2): 151–170.
[26] Fox M, Agarwal K, Shinmura T, Komanduri R (1994) Magnetic abrasive finishing of rollers.Ann CIRP 43: 181–184.

[27] Komanduri R (1996) On material removal mechanism in finishing of advanced ceramics and glasses. Ann CIRP 45(1): 509–514.
[28] Singh DK, Jain VK, Raghuram V (2004) Parametric study of magnetic abrasive finishing process. J Mater Process Technol 149: 22–29.
[29] Jain VK, Kumar P, Behra PK, Jayswal SC (2001a) Effect of working gap and circumferential speed on the performance of magnetic abrasive finishing process. Wear 250: 384–390.
[30] Tani Y, Kawata K (1984) Development of high efficient fine finishing process using magnetic fluid. Ann CIRP 33(1): 377–381.
[31] Umehara N (1994) Magnetic fluid grinding – A new technique for finish advanced ceramics. Ann CIRP 43(1): 85–188.
[32] Kim JD (1997) Development of magnetic abrasive jet machining system for internal polishing of circular tubes. J Mater Process Technol 71: 384–393.